

Received October 16, 2020, accepted October 26, 2020, date of publication October 29, 2020, date of current version November 11, 2020.

Digital Object Identifier 10.1109/ACCESS.2020.3034760

Efficient Rigorous Coupled-Wave Analysis Without Solving Eigenvalues for Analyzing One-Dimensional Ultrathin Periodic Structures

JIE LI^{ID}, JIAN-BAO WANG^{ID}, ZHENG SUN, LI-HUA SHI^{ID}, (Member, IEEE), YAO MA^{ID},
QI ZHANG^{ID}, SHANG-CHEN FU^{ID}, YI-CHENG LIU^{ID}, AND YU-ZHOU RAN^{ID}

National Key Laboratory on Electromagnetic Environmental Effects and Electro-Optical Engineering, Army Engineering University of PLA, Nanjing 210007, China

Corresponding author: Jian-Bao Wang (zwang0417@outlook.com)

This work was supported by the National Natural Science Foundation of China under Grant 51977219.

ABSTRACT Based on the first-order Taylor expansion, an efficient Rigorous Coupled-Wave Analysis (RCWA) for one-dimensional ultrathin periodic structures is proposed in this paper. The derivation of the ultrathin form RCWA method is completed by using the first-order Taylor expansion to rearrange the matrix in the equations of boundary conditions. Then, the reliability of the proposed algorithm is verified by two examples. Finally, it is concluded that the proposed algorithm can reduce the CPU time of TE polarization and TM polarization by more than 50%. Meanwhile, compared with the conventional algorithm, the proposed algorithm also needs less memory.

INDEX TERMS RCWA, eigenvalues and eigenvectors, computational efficiency, ultrathin periodic structures.

I. INTRODUCTION

Periodic structures, which are widely applied in frequency selective surfaces (FSSs), metasurfaces, and so on, are the most universal and aesthetic structure in nature. In the study of the interaction between electromagnetic waves and periodic structures, a variety of analytical or numerical electromagnetic calculation methods have been proposed. Numerical methods can generally be divided into time-domain methods and frequency-domain methods, such as FDTD [1], [2] and FDFD [3], [4]. These methods have certain universality, but for some specific structures, other methods have more advantages in efficiency and accuracy. For example, among the existing methods for analyzing electromagnetic field scattering problems of one-dimensional periodic structures, RCWA is the most successful and widely used one [5]–[10]. For improving the poor convergence of RCWA, Li and Lalanne *et al.* rearranged Maxwell's curl equations and proposed the Inverse rule [11]–[13]. Evgeny Popov and Schuster *et al.* proposed the NV method by decomposing the electromagnetic field [14], [15]. To improve the computational efficiency, S. Peng *et al.* proposed an efficient

RCWA method, which reduces the eigenvalue problem of the grating in a conical mounting to two eigenvalue problems in the corresponding nonconical mounting [16]. I. Semenikhin *et al.* improved the computational efficiency of RCWA by using a series of auxiliary equations [17]. By combining RCWA with the perturbation method, Edee *et al.* avoided the repeated calculation of eigenvalues of multilayer gratings [18], [19].

However, for one-dimensional ultrathin periodic structures, especially ultrathin metallic gratings, the conventional RCWA method have such shortcomings as low efficiency and needs large memory. Besides, when the accuracy is high and the truncation orders are large, how to solve the eigenvalues of the super-large eigenmatrix is also a difficult problem that restricts the further development of this method. Therefore, it is necessary to develop simple and efficient algorithms for one-dimensional ultrathin periodic structures. Different articles have contributed to this. For zero-thickness gratings, Wakabayashi *et al.* [20] put forward that surface relief dielectric gratings with various profiles can be treated as a plane grating with surface impedance functioning as of the position parameter. Lalanne and Lemerrier-Lalanne *et al.* [21] improved the convergence by using the second-order Taylor expansion. At the same time, he also gave the

The associate editor coordinating the review of this manuscript and approving it for publication was Davide Comite^{ID}.

closed-form expression of the effective indices of ultrathin gratings based on the equivalent medium theory. It is worth noting that the work of Wakabayashi *et al.* [20] is only applicable to dielectric surface-relief gratings, while ultrathin metallic surface-relief gratings cannot be replaced by plane gratings with surface impedance. Lalanne and Lemercier-Lalanne [21] only gave the approximate expression of TE polarization incidence while TM polarization incidence does not apply to this theory. Further studies are needed on one-dimensional ultrathin periodic structures.

In this paper, based on the first-order Taylor expansion, an efficient algorithm that can be used for one-dimensional ultrathin periodic structures is proposed. In section II, for better introducing this method, a brief introduction about RCWA and the geometry used in this paper are presented. In this section, the notations and some equations can be found in [10]. In Section III, for one-dimensional ultrathin periodic structures, based on the first-order Taylor expansion, the equations of boundary conditions are reformulated by using the sum of two simple diagonal matrices to take the place of the exponential matrix. After that, a new method for solving the equations of boundary conditions is proposed. This new method involves nor eigenvalues or eigenvectors. Section IV provides numerical evidence that the new method significantly improves efficiency. Discussion and concluding remarks are given in Section V and Section VI respectively.

II. GEOMETRY AND CONVENTIONAL METHOD

The geometry of the grating diffraction problem is depicted in Fig. 1. The grating periodic along the x -direction with a relative permittivity $\varepsilon^r(x)$. The z -axis is perpendicular to the boundaries, and the diffraction problem is invariant in the y -direction. The grating region is bound by two different media with relative permittivity ε_1 and ε_2 , and the permeability is μ_0 . The period of the structure is denoted by Λ , its depth is d , f denotes duty cycle, and the length of the grating vector K is equal to $2\pi/\Lambda$. θ denotes the angle of the incident wave.

TE polarization is taken as an example in this section, and extension to TM polarization is quite simple. The periodic relative permittivity of the grating region ($0 < z < d$) can be expanded to a Fourier series of the form as

$$\varepsilon^r(x) = \sum_{h=-\infty}^{+\infty} \varepsilon_h^r e^{jKhx}, \quad (1)$$

where ε_h^r is the h th Fourier coefficient of $\varepsilon^r(x)$.

Using the space harmonic expansion, the tangential electric field E_{gy} and magnetic field H_{gx} in the grating region may be expressed as

$$E_{gy} = \sum_{i=-\infty}^{+\infty} S_{yi}(z) e^{-jk_{xi}x}, \quad (2)$$

$$H_{gx} = -j\sqrt{\frac{\varepsilon_0}{\mu_0}} \sum_{i=-\infty}^{+\infty} U_{xi}(z) e^{-jk_{xi}x}, \quad (3)$$

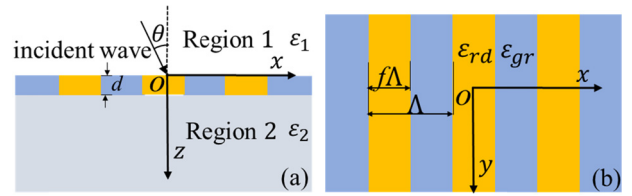


FIGURE 1. Geometry for the grating diffraction problem. (a) front view, (b) top view.

where S_{yi} and U_{xi} represent the normalized amplitudes of the i th space harmonic fields of E_{gy} and H_{gx} respectively, and j is the imaginary unit. k_{xi} is determined from the Floquet condition and is provided by

$$k_{xi} = k_0 n_1 \sin \theta - iK. \quad (4)$$

where k_0 is the wavenumber in air, and n_1 is the square root of ε_1 .

Maxwell's curl equations in the grating region are

$$\frac{\partial E_{gy}}{\partial z} = j\omega\mu_0 H_{gx}, \quad (5)$$

$$\frac{\partial H_{gx}}{\partial z} - \frac{\partial H_{gz}}{\partial x} = j\omega\varepsilon_0 \varepsilon^r(x) E_{gy}. \quad (6)$$

In the actual calculation process, it is necessary to truncate the Fourier expansion of relative permittivity $\varepsilon^r(x)$ and space harmonic expansion of the tangential electric field E_{gy} and magnetic field H_{gx} in the grating region. Suppose the truncation order is N , then substituting (2) and (3) into (5) and (6) and eliminating H_{gz} , the coupled-wave equations in matrix form can be expressed as

$$\left[\frac{\partial^2 S_y}{\partial (z')^2} \right] = [A] [S_y], \quad (7)$$

where $z' = k_0 z$ and

$$[A] = [K_x^2] - [E], \quad (8)$$

where K_x is an $N \times N$ diagonal matrix with the elements k_{xi}/k_0 , and E is an $N \times N$ Toeplitz matrix with the i, p element being equal to ε_{i-p}^r .

Solving the eigen equation, S_{yi} and U_{xi} are then given by

$$S_{yi}(z) = \sum_{m=1}^N w_{i,m} \left\{ e^{-k_0 q_m z} \cdot c_m^+ + e^{k_0 q_m (z-d)} \cdot c_m^- \right\}, \quad (9)$$

$$U_{xi}(z) = \sum_{m=1}^N v_{i,m} \left\{ -e^{-k_0 q_m z} \cdot c_m^+ + e^{k_0 q_m (z-d)} \cdot c_m^- \right\}, \quad (10)$$

where $w_{i,m}$ and q_m are the components of eigenvector matrix $[W]$ and diagonal matrix $[Q]$ composed by positive square roots of eigenvalues of matrix $[A]$, respectively. The formula $v_{i,m}$ is the element of matrix $[V]$, where $[V] = [W][Q]$. The quantities c_m^+ and c_m^- are unknown constants to be determined from the boundary conditions.

By matching the tangential electric- and magnetic-field components at boundaries $z = 0$ and $z = d$, the following matrix equations can be obtained

$$\begin{bmatrix} \delta_{i0} \\ jn_1 \cos \theta \delta_{i0} \end{bmatrix} + \begin{bmatrix} I \\ -jY_I \end{bmatrix} [R] = \begin{bmatrix} W & WX \\ V & -VX \end{bmatrix} \begin{bmatrix} c^+ \\ c^- \end{bmatrix}, \quad (11)$$

$$\begin{bmatrix} I \\ jY_{II} \end{bmatrix} [T] = \begin{bmatrix} WX & W \\ VX & -V \end{bmatrix} \begin{bmatrix} c^+ \\ c^- \end{bmatrix}, \quad (12)$$

where $[X]$ is a diagonal matrix with the diagonal elements $\exp(-k_0 q_m d)$. $[Y_I]$, $[Y_{II}]$ are $N \times N$ diagonal matrices with elements $k_{1,zi}/k_0$, and $k_{2,zi}/k_0$ and

$$k_{l,zi} = \begin{cases} (k_0^2 n_l^2 - k_{xi}^2)^{0.5}, & k_0 n_l > k_{xi} \\ -j(k_{xi}^2 - k_0^2 n_l^2)^{0.5}, & k_0 n_l < k_{xi}, \end{cases} \quad l = 1, 2, \quad (13)$$

$[I]$ is an identity matrix, $\delta_{i0} = 1$ for $i = 0$, and $\delta_{i0} = 0$ for $i \neq 0$. The forward- and backward-diffracted amplitudes T_i and R_i can be got by solving (11) and (12) simultaneously. However, because of possible zero columns on the right-hand sides of (11) and (12), which is caused by very small terms in the diagonal matrix $[X]$ when some of the generally complex eigenvalues have a large positive real part, attempts to solve (12) for $[c^+]$ and $[c^-]$ in terms of $[T]$ and then substitute for $[c^+]$ and $[c^-]$ in (11) to determine $[T]$ and $[R]$ will probably cause numerical instability [10].

In this paper, the original complex exponential term matrix is transformed into the sum of two simple matrices by using the first-order Taylor expansion. Then the rearranged equations of boundary conditions not only improve the computational efficiency but also solve the problem that TM polarization is not applicable.

III. NEW FORMULATION OF THE PROPOSED METHOD

In this section, a new method will be proposed to implement the coupled-wave formulation. For one-dimensional ultrathin periodic structures, the proposed method can effectively reduce the number of operations and the operation time. Generally, when $k_0 d \ll 1$, it can be regarded as ultrathin. Equation (14) gives the rigorous conditions that d should satisfy, more details can be found in the Appendix.

$$d \leq \left| \frac{a + bj}{2\pi \sqrt{Nn_1^2 \sin^2 \theta + \frac{\lambda_0^2}{\Lambda^2} \frac{m(m+1)(m+2)}{3} - N\epsilon_0^r}} \right| \lambda_0 \quad (14)$$

Considering ultrathin structures and q_m is a finite value, so according to the first-order Taylor expansion, $\exp(\pm k_0 q_m d)$ can be expanded as

$$e^{\pm k_0 q_m d} \sim 1 \pm k_0 q_m d. \quad (15)$$

Therefore, matrix $[X]$ can be replaced by

$$[X] = [I] - k_0 d [Q], \quad (16)$$

where $[Q]$ is a diagonal matrix with the elements q_m .

Similarly,

$$[X]^{-1} = [I] + k_0 d [Q]. \quad (17)$$

According to (16) and (17), there are

$$[W] [X^{-1} + X] [W]^{-1} = 2[I], \quad (18)$$

$$[W] [X^{-1} - X] [V]^{-1} = 2k_0 d [I], \quad (19)$$

$$[V] [X^{-1} + X] [V]^{-1} = 2[I], \quad (20)$$

$$[V] [X^{-1} - X] [W]^{-1} = 2k_0 d [W] [Q]^2 [W]^{-1}. \quad (21)$$

Using (12), the equation can be rewritten as

$$\begin{bmatrix} X^{-1} \\ X \end{bmatrix} \begin{bmatrix} W & W \\ V & -V \end{bmatrix}^{-1} \begin{bmatrix} I \\ jY_{II} \end{bmatrix} [T] = \begin{bmatrix} I & \\ & X \end{bmatrix} \begin{bmatrix} c^+ \\ c^- \end{bmatrix}. \quad (22)$$

Besides, (11) can be rewritten as

$$\begin{bmatrix} \delta_{i0} \\ jn_1 \cos \theta \delta_{i0} \end{bmatrix} + \begin{bmatrix} I \\ -jY_I \end{bmatrix} [R] = \begin{bmatrix} W & W \\ V & -V \end{bmatrix} \begin{bmatrix} I & \\ & X \end{bmatrix} \begin{bmatrix} c^+ \\ c^- \end{bmatrix}. \quad (23)$$

Substituting (22), and (18)-(21) into (23), it may be reformulated as

$$\begin{bmatrix} \delta_{i0} \\ jn_1 \cos \theta \delta_{i0} \end{bmatrix} + \begin{bmatrix} I \\ -jY_I \end{bmatrix} [R] = \begin{bmatrix} I & k_0 d I \\ M & I \end{bmatrix} \begin{bmatrix} I \\ jY_{II} \end{bmatrix} [T], \quad (24)$$

where

$$[M] = k_0 d [W] [Q]^2 [W]^{-1}. \quad (25)$$

According to the relationship between matrix $[W]$ and $[Q]$ and eigenmatrix $[A]$, there is

$$[W] [Q]^2 [W]^{-1} = [A]. \quad (26)$$

Therefore, (25) can be rewritten as

$$[M] = k_0 d [A]. \quad (27)$$

Thus, matrix $[M]$ is only related to eigenmatrix $[A]$ rather than eigenvectors matrix $[W]$ or eigenvalues matrix $[Q]$. By solving (24), $[R]$ and $[T]$ can be calculated from the eigenmatrix rather than its eigenvalues and eigenvectors, which avoids numerical instability due to some of the generally complex eigenvalues have a large positive real part as mentioned in section II.

For convenience, (24) is replaced by the following expression

$$[A_1] + [A_2] [R] = [A_3] [A_4] [T], \quad (28)$$

where

$$[A_1] = \begin{bmatrix} \delta_{i0} \\ jn_1 \cos \theta \delta_{i0} \end{bmatrix}, \quad (29)$$

$$[A_2] = \begin{bmatrix} I \\ -jY_I \end{bmatrix}, \quad (30)$$

$$[A_3] = \begin{bmatrix} I & k_0 d I \\ M & I \end{bmatrix}, \quad (31)$$

$$[A_4] = \begin{bmatrix} I \\ jY_{II} \end{bmatrix}. \quad (32)$$

To calculate the reflection and transmission amplitudes of each diffraction order, (28) is rearranged to

$$\begin{bmatrix} T \\ R \end{bmatrix} = [A_3 A_4 - A_2]^{-1} [A_1]. \quad (33)$$

Then the diffraction efficiency of each diffraction order can be obtained by using

$$\begin{aligned} DE_{ri} &= R_i R_i^* \operatorname{Re} \left(\frac{k_{1,zi}}{k_0 n_1 \cos \theta} \right), \\ DE_{ti} &= T_i T_i^* \operatorname{Re} \left(\frac{k_{2,zi}}{k_0 n_1 \cos \theta} \right), \end{aligned} \quad (34)$$

where DE_{ri} and DE_{ti} represent the forward and backward diffraction efficiency of each order respectively, R_i^* and T_i^* denotes the conjugate amplitudes of the diffracted fields R_i and T_i . Conservation of energy without loss is defined by

$$\sum_i DE_{ri} + DE_{ti} = 1 \quad (35)$$

and is a necessary criterion for the numerical stability of the algorithm. It must be remembered that satisfying the power conservation condition does not guarantee the accuracy of the diffraction efficiency of each diffraction order. The accuracy of the individual diffraction efficiency depends on the number of space harmonics retained in the field expansions. The higher the truncation order, the higher the accuracy of the individual diffraction efficiency.

By using (22), $[c^+]$ and $[c^-]$ are directly substituted into (11), which avoids the numerical instability of replacing $[c^+]$ and $[c^-]$ with $[T]$ to solve $[R]$ in (11). Through the above derivation, the forward and backward diffraction efficiency of each order can be solved using the eigenmatrix rather than eigenvalues and eigenvectors.

IV. NUMERICAL VALIDATION

To validate the accuracy and the efficiency of the proposed algorithm, two examples are selected to compare the calculation results of the conventional method proposed in [10], the proposed method of this paper, and the CST simulations respectively. The binary grating is a classic example that has been analyzed by many papers. Considering that this structure is a one-dimensional periodic structure, thus an ultrathin binary grating is chosen as the first example to verify the performance of the proposed method. Thereinto, the numerical results obtained by the traditional RCWA method [10] and CST simulations are used as a benchmark for comparison. Moreover, to furthering certify the accuracy of and proving the applicability of the proposed method, a Frequency Selective Surface which is a mixture of metal and media is analyzed in the second example.

A. RECTANGLE ULTRATHIN BINARY GRATING

Consider a rectangle ultrathin binary grating depicted in Fig. 1. Region 1 is air and region 2 is FR4 with $\epsilon_2 = 3.75$. The period of the structure Λ is 1 cm, f is 0.5 and the grating depth d is 100 μm . In the grating region, $\epsilon_{gr} = 1$. The grating

structure is medium with relative permittivity $\epsilon_r = 1$ and conductivity $\sigma = 5 \times 10^3 \text{ S/m}$. The incident angle θ is 0 degrees, 30 degrees, and 60 degrees. Fig. 2 shows the transmission efficiency of TE and TM polarization in the case of truncation orders $N = 301$, which include forward diffraction efficiency of all orders. The simulation information of the two methods under 30 degrees incidence is shown in Table 1, and the memory listed in Table 1 is obtained when $N = 301$.

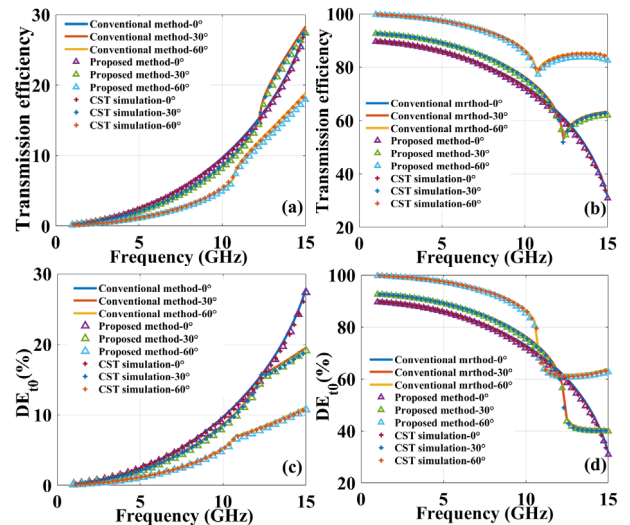


FIGURE 2. The transmission efficiency and 0-order diffraction efficiency of example 1. ((a) Transmission efficiency of TE polarization, (b) transmission efficiency of TM polarization. (c) The 0-order diffraction efficiency of TE polarization, (d) 0-order diffraction efficiency of TM polarization. Solid line, the conventional method. Triangular, the proposed method. Cross, the CST simulations).

TABLE 1. The simulation information of two algorithms (processor: Intel Core CPU I 7-7700 3.6GHz, operating system: Microsoft Windows 10, programming language: MATLAB, time unit: s, memory unit: MB).

| Method | | Memory | | | | Time (truncation order is N) | | | |
|--------------|----|---------|------|------|-------|---------------------------------|-----|-----|-----|
| | | $N=301$ | 101 | 201 | 301 | $N=301$ | 101 | 201 | 301 |
| Conventional | TE | 98.3 | 1.80 | 7.36 | 17.90 | | | | |
| | TM | 83.6 | 1.82 | 7.93 | 18.72 | | | | |
| Proposed | TE | 49.7 | 0.82 | 3.07 | 7.01 | | | | |
| | TM | 40.2 | 0.88 | 3.31 | 7.78 | | | | |

B. FREQUENCY SELECTIVE SURFACE

The second example is a Frequency Selective Surface (FSS) which is one of the metasurfaces that can be used as spatial filters to transmit or reflect electromagnetic waves with different operating frequencies, polarizations, and incident angles. In the following, the diffraction problem of an FSS consisting of metallic gold and silica under TE polarization will be considered. The geometry and related parameters of the FSS are shown in Fig. 3. Table 2 shows that, compared with the conventional method, the proposed method has greatly improved both in computational efficiency and

memory, which is consistent with the conclusion in example 1. In this example, there is more than one propagating order due to the wavelength of the incident field (3.33-10 mm) is smaller than the period of the structure ($\Lambda = 10$ mm). As can be seen from Fig. 4 that under normal incident, when the frequency is greater than 60 GHz, the positive second-order begins to propagate and the ratio of the period to wavelength is greater than 2. Likewise, negative first order and negative second-order begin to propagate when the frequency is greater than 30 GHz, and 60 GHz respectively.

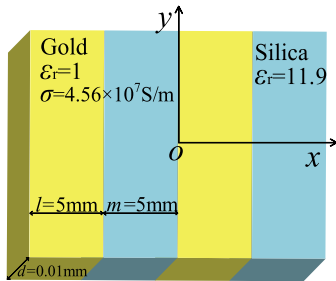


FIGURE 3. Geometry of the FSS considered in this paper.

TABLE 2. The simulation information of example 2 (processor: Intel Core CPU I 7-7700 3.6GHz, operating system: Microsoft Windows 10, programming language: MATLAB, time unit: s, memory unit: MB).

| Method | Memory | Time (truncation order is N) | | |
|--------------|---------|---------------------------------|------|-------|
| | $N=301$ | 101 | 201 | 301 |
| Conventional | 89.7 | 1.58 | 7.11 | 17.52 |
| Proposed | 41.5 | 0.85 | 3.57 | 8.67 |

V. DISCUSSION

It can be seen from Fig. 2 and Fig. 4 that the calculation results of the proposed method, the conventional method, and the CST simulations have good consistency in both TE polarization and TM polarization, indicating that the proposed method is reliable. Comparing the calculation time in Table 1 and Table 2, it is obvious that the proposed algorithm can save more than 50% CPU time. This is mainly because for one-dimensional ultrathin periodic structures, the proposed method involves nor eigenvalues or eigenvectors, and the diffraction efficiency is directly solved from the eigenmatrix. Thus, the time-consuming problem of solving eigenvalues and eigenvectors is effectively avoided. It is not difficult to draw from the above results that compared with the conventional RCWA method, the proposed method has the following advantages,

a. Simpler executive equations. Compared with the conventional method, the proposed method of this paper owns simpler executive equations. T_i and R_i can be calculated by using (33) rather than solving a series of complex-linear boundary conditions equations.

b. Less memory. The proposed method does not need to solve eigenvalues and eigenvectors, nor store their values, which reduces the memory requirements. Besides, from the

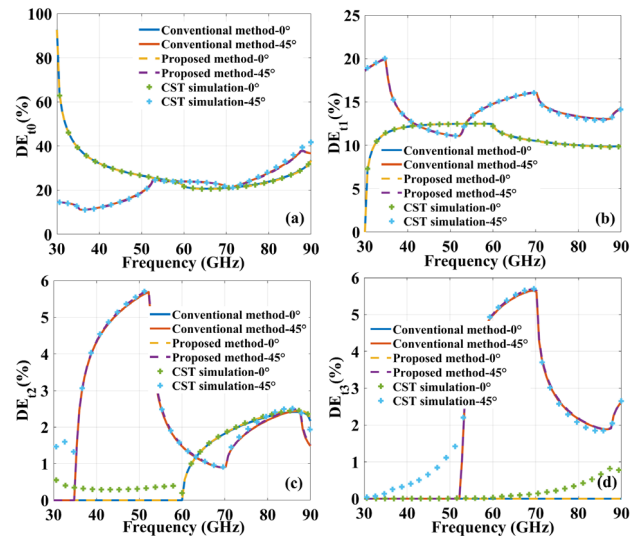


FIGURE 4. The forward diffraction efficiency of each order. (a), DE_{10} . (b), DE_{11} . (c), DE_{12} . (d), DE_{13} . Blue solid line, 0 degrees of the conventional method. Brown solid line, 45 degrees of the conventional method. Yellow dotted line, 0 degrees of the proposed method. Purple dotted line, 45 degrees of the proposed method. Green cross, 0 degrees of the CST simulations. Blue cross, 45 degrees of the CST simulations).

comparison of (11) and (12) and (33), the proposed method significantly reduces the storage of intermediate variables, which will also reduce the demand for memory. This conclusion can be drawn more clearly from the data comparison of Table 1 and Table 2.

c. More efficient. The proposed method uses two simple diagonal matrices to replace the exponential matrix so that there is no need to solve the eigenvalues and eigenvectors of the eigenmatrix when calculating the forward- and backward-diffracted amplitudes T_i and R_i . Generally, the larger the N , the longer the computational time required by the RCWA method, and the computational time proportional to N^3 . From the data provided in Table 1 and Table 2, compared with the conventional method, the proposed method can save more than 50% CPU time.

VI. CONCLUSION

In this paper, based on the first-order Taylor expansion, an algorithm for one-dimensional ultrathin periodic structures with higher efficiency and fewer memory requirements is proposed. The proposed algorithm solves the forward and backward diffraction efficiency by using the eigenmatrix rather than eigenvalues and eigenvectors, which avoids the time-consuming problem of solving eigenvalues and greatly improves computational efficiency. The numerical results show that the results of the proposed method are in good agreement with those obtained by the traditional RCWA method [10] and the CST simulations in different cases.

The algorithm proposed in this paper is not only suitable for dielectric and metallic ultrathin binary gratings, but also other one-dimensional ultrathin periodic structures. Also, we hope this method will be extended to two-dimensional

ultrathin periodic structures and metasurfaces in future research.

APPENDIX

In the following, a specific derivation on the condition that the thickness d can be regarded as ultrathin will be made.

According to the relationship between eigenvalue and eigenmatrix, there is

$$\lambda_1 + \lambda_2 + \lambda_3 + \dots + \lambda_N = \sum_{i=1}^N a_{ii} \quad (36)$$

where λ_i and a_{ii} are the i th eigenvalue and the i, i element of eigenmatrix $[A]$ respectively.

A. THE CONDITION THAT THE PROPOSED METHOD DEVIATES FROM THE CONVENTIONAL METHOD

Using (36), there is

$$N\lambda_{\max} \geq \sum_{i=1}^N a_{ii} \quad (37)$$

where λ_{\max} denotes the maximum value of λ_i .

Substituting (8) into (37), the following equation can be got

$$N\lambda_{\max} \geq \sum_{i=-m}^m \left(\frac{k_{xi}}{k_0}\right)^2 - N\epsilon_0^r \quad (38)$$

Substituting (4) into (38), the following equation can be got

$$N\lambda_{\max} \geq \sum_{i=-m}^m \left(n_1^2 \sin^2 \theta - 2\frac{\lambda_0}{\Lambda} n_1 \sin \theta i + \frac{\lambda_0^2}{\Lambda^2} i^2\right) - N\epsilon_0^r \quad (39)$$

where λ_0 is the wavelength in air and $N = 2m + 1$.

Equation (39) can be simplified as

$$N\lambda_{\max} \geq Nn_1^2 \sin^2 \theta + 2\frac{\lambda_0^2}{\Lambda^2} \sum_{i=1}^m i^2 - N\epsilon_0^r \quad (40)$$

Namely

$$\lambda_{\max} \geq n_1^2 \sin^2 \theta + \frac{\lambda_0^2}{\Lambda^2} \frac{m(m+1)(m+2)}{3N} - \epsilon_0^r \quad (41)$$

So, according to (41), the minimum value of λ_{\max} is

$$(\lambda_{\max})_{\min} = n_1^2 \sin^2 \theta + \frac{\lambda_0^2}{\Lambda^2} \frac{m(m+1)(m+2)}{3N} - \epsilon_0^r \quad (42)$$

and the minimum value of q_{\max} is

$$(q_{\max})_{\min} = \sqrt{n_1^2 \sin^2 \theta + \frac{\lambda_0^2}{\Lambda^2} \frac{m(m+1)(m+2)}{3N} - \epsilon_0^r} \quad (43)$$

where min denotes the minimum value.

As we knew, the closer x is to 0, the smaller the error of replacing $\exp(x)$ with $1+x$ is. Supposed that when $|k_0dq|$ is greater than $|a + bj|$, $1 + k_0dq$ can no longer be used to take the place of $\exp(k_0dq)$. So when

$$|k_0(q_{\max})_{\min}d| > |a + bj| \quad (44)$$

Namely

$$\left|k_0d\sqrt{n_1^2 \sin^2 \theta + \frac{\lambda_0^2}{\Lambda^2} \frac{m(m+1)(m+2)}{3N} - \epsilon_0^r}\right| > |a + bj| \quad (45)$$

According to (45), the range of thickness d can be got

$$d > \left| \frac{a + bj}{2\pi\sqrt{n_1^2 \sin^2 \theta + \frac{\lambda_0^2}{\Lambda^2} \frac{m(m+1)(m+2)}{3N} - \epsilon_0^r}} \right| \lambda_0 \quad (46)$$

Under this condition, the calculation results of the proposed method deviate from those of the conventional method.

B. THE CONDITION THAT THE THICKNESS D CAN BE REGARDED AS ULTRATHIN

In the actual calculation process, λ_i is always greater than 0, so (36) can be rewritten as

$$\lambda_{\max} \leq \sum_{i=1}^N a_{ii} \quad (47)$$

Namely

$$\lambda_{\max} \leq \sum_{i=-m}^m \left(\frac{k_{xi}}{k_0}\right)^2 - N\epsilon_0^r \quad (48)$$

Substituting (4) and (8) into (48), it can be rewritten as

$$\lambda_{\max} \leq Nn_1^2 \sin^2 \theta + \frac{\lambda_0^2}{\Lambda^2} \frac{m(m+1)(m+2)}{3} - N\epsilon_0^r \quad (49)$$

So, according to (49), the minimum value of λ_{\max} is

$$(\lambda_{\max})_{\max} = Nn_1^2 \sin^2 \theta + \frac{\lambda_0^2}{\Lambda^2} \frac{m(m+1)(m+2)}{3} - N\epsilon_0^r \quad (50)$$

and the maximum value of q_{\max} is

$$(q_{\max})_{\max} = \sqrt{Nn_1^2 \sin^2 \theta + \frac{\lambda_0^2}{\Lambda^2} \frac{m(m+1)(m+2)}{3} - N\epsilon_0^r} \quad (51)$$

where max denotes the maximum value.

Contrary to part A, when $|k_0dq|$ is smaller than $|a + bj|$, $1 + k_0dq$ can be used to take the place of $\exp(k_0dq)$. Namely

$$|k_0(q_{\max})_{\max}d| \leq |a + bj| \quad (52)$$

Using (52), we can get

$$d \leq \left| \frac{a + bj}{2\pi\sqrt{Nn_1^2 \sin^2 \theta + \frac{\lambda_0^2}{\Lambda^2} \frac{m(m+1)(m+2)}{3} - N\epsilon_0^r}} \right| \lambda_0 \quad (53)$$

Under this condition, the calculation results of the proposed method are in good agreement with those of the conventional method.

Different values of a and b correspond to different calculation accuracy. The higher the accuracy requirements are, the closer the values of a and b are to 0. Generally, when a and b are equal to 0.1, the accuracy requirements can be met.

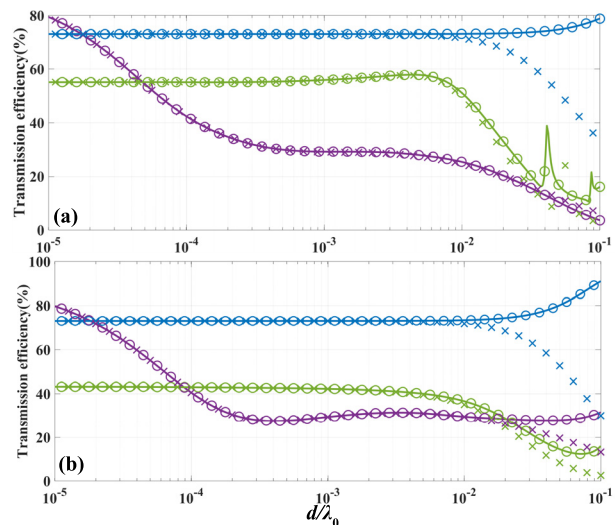


FIGURE 5. The influence of the ratio of thickness to wavelength on the results of the two methods under different parameters. (a) TE polarization, (b) TM polarization solid line, the conventional method. Circle, the CST simulation. Cross, the proposed method. Purple, Green, and Blue represent examples 1, 2, and 3 respectively.)

C. SIMULATION RESULTS

In the foregoing work, the condition that the thickness d can be regarded as ultrathin is derived analytically. Next, three simulation examples are used to show this condition more clearly. In the simulation process, it is assumed that θ is 0 degrees. The related parameters of examples 1 and 2 correspond to the two numerical examples in Section IV, and the frequency of 15 GHz and 90 GHz are chosen as the reference respectively. The third example is a grating with $\epsilon_1 = 1$ and $\epsilon_2 = 10$ respectively. In the grating region, the relative permittivity $\epsilon_{rd} = 10$ and $\epsilon_{gr} = 1$, and it is assumed that λ_0 and Λ are 1 cm, f is 0.5. Fig. 5 shows the transmission efficiency of three examples under different ratios of thickness to wavelength.

It can be seen from Fig. 5 that when d is less than $10^{-3}\lambda_0$, the calculation results of the conventional method, the CST simulation, and the proposed method are consistent. In this case, from a numerical point of view, d can be considered as ultrathin. As d continues to increase, there will be differences between the proposed method, the conventional method, and CST simulation results. But, when d is less than $10^{-2}\lambda_0$, the difference between the calculation results of the three methods is still very small. By substituting the parameters of the three examples into (46) and (53), it can be concluded that, when d is greater than $10^{-3.74}\lambda_0$, $10^{-5.01}\lambda_0$, and $10^{-3.43}\lambda_0$, the results of the two methods will begin to show differences. When d is less than $10^{-4.98}\lambda_0$, $10^{-6.25}\lambda_0$, and $10^{-4.67}\lambda_0$, the results of the two methods are in high agreement. From the comparison between the theoretical derivation and the simulation results, it can be found that the conditions of the theoretical derivation are more stringent than the simulation results, which means that in the actual calculation process, we can appropriately take larger a and b as the condition to judge whether the d can be regarded as ultrathin. Usually,

when d is less than $10^{-3}\lambda_0$, the calculation results of the proposed method can meet the requirements. Of course, if the requirement of numerical accuracy is reduced, when d is less than $10^{-2}\lambda_0$, it can also be regarded as ultrathin, and the proposed method can be used for more efficient calculation.

REFERENCES

- [1] J. Wang, B. Zhou, L. Shi, C. Gao, and B. Chen, "A novel 3-D HIE-FDTD method with one-step leapfrog scheme," *IEEE Trans. Microw. Theory Techn.*, vol. 62, no. 6, pp. 1275–1283, Jun. 2014.
- [2] Y. Liu, L. Shi, J. Wang, H. Chen, Q. Lei, Y. Duan, Q. Zhang, S. Fu, and Z. Sun, "TO-FDTD method for arbitrary skewed periodic structures at oblique incidence," *IEEE Trans. Microw. Theory Techn.*, vol. 68, no. 2, pp. 564–572, Feb. 2020.
- [3] T. T. Koutserimpas, A. D. Papadopoulos, and E. N. Glytsis, "Applicability and optimization of the alternating-direction-implicit iterative method for the 2-D finite-difference frequency-domain solution of scattering problems," *IEEE Trans. Antennas Propag.*, vol. 65, no. 12, pp. 7166–7173, Dec. 2017.
- [4] K. Masumnia-Bisheh, K. Forooghi, and M. Ghaffari-Miab, "Electromagnetic uncertainty analysis using stochastic FDFD method," *IEEE Trans. Antennas Propag.*, vol. 67, no. 5, pp. 3268–3277, May 2019.
- [5] B. J. Civiletti, A. Lakhtakia, and P. B. Monk, "Analysis of the rigorous coupled wave approach for s-polarized light in gratings," *J. Comput. Appl. Math.*, vol. 368, Apr. 2020, Art. no. 112478.
- [6] Y. Shahamat, A. Ghaffarinejad, and M. Vahedi, "Enhancement of light absorption in photocatalytic devices with multilayered ultra-thin silver elements," *Opt. Commun.*, vol. 450, pp. 228–235, Nov. 2019.
- [7] C. S. Wan, T. K. Gaylord, and M. S. Bakir, "RCWA-EIS method for interlayer grating coupling," *Appl. Opt.*, vol. 55, no. 22, pp. 5900–5908, Aug. 2016.
- [8] S. T. Peng, T. Tamir, and H. L. Bertoni, "Theory of periodic dielect waveguides," *IEEE Trans. Microw. Theory Techn.*, vol. 23, no. 1, pp. 123–133, Jan. 1975.
- [9] M. G. Moharam and T. K. Gaylord, "Rigorous coupled-wave analysis of metallic surface-relief gratings," *J. Opt. Soc. Amer. A, Opt. Image Sci.*, vol. 3, no. 11, pp. 1780–1787, Nov. 1986.
- [10] M. G. Moharam, E. B. Grann, D. A. Pommet, and T. K. Gaylord, "Formulation for stable and efficient implementation of the rigorous coupled-wave analysis of binary gratings," *J. Opt. Soc. Amer. A, Opt. Image Sci.*, vol. 12, no. 5, pp. 1068–1076, 1995.
- [11] L. F. Li and C. W. Haggans, "Convergence of the coupled-wave method for metallic lamellar diffraction gratings," *J. Opt. Soc. Amer. A, Opt. Image Sci.*, vol. 10, no. 6, pp. 1184–1189, Jun. 1993.
- [12] P. Lalanne and G. M. Morris, "Highly improved convergence of the coupled-wave method for TM polarization," *J. Opt. Soc. Amer. A, Opt. Image Sci.*, vol. 13, no. 4, pp. 779–784, Apr. 1996.
- [13] L. Li, "Use of Fourier series in the analysis of discontinuous periodic structures," *J. Opt. Soc. Amer. A, Opt. Image Sci.*, vol. 13, no. 9, pp. 1870–1876, Sep. 1996.
- [14] E. Popov and M. Neviere, "Maxwell equations in Fourier space: Fast-converging formulation for diffraction by arbitrary shaped, periodic, anisotropic media," *J. Opt. Soc. Amer. A, Opt. Image Sci.*, vol. 18, no. 11, pp. 2886–2894, Nov. 2001.
- [15] T. Schuster, J. Ruoff, N. Kerwien, S. Rafler, and W. Osten, "Normal vector method for convergence improvement using the RCWA for crossed gratings," *J. Opt. Soc. Amer. A, Opt. Image Sci.*, vol. 24, no. 9, pp. 2880–2890, Sep. 2007.
- [16] S. Peng and G. M. Morris, "Efficient implementation of rigorous coupled-wave analysis for surface-relief gratings," *J. Opt. Soc. Amer. A, Opt. Image Sci.*, vol. 2532, no. 5, pp. 475–480, 1995.
- [17] I. Semenikhin, M. Zanucoli, M. Benzi, V. Vyurkov, E. Sangiorgi, and C. Fiegna, "Computational efficient RCWA method for simulation of thin film solar cells," *Opt. Quantum Electron.*, vol. 44, nos. 3–5, pp. 149–154, Jun. 2012.
- [18] K. Edee, J. P. Plumey, G. Granet, and J. Hazart, "Perturbation method for the Rigorous Coupled Wave Analysis of grating diffraction," *Opt. Express*, vol. 18, no. 25, pp. 26274–26284, Dec. 2010.
- [19] J. Bischoff and K. Hehl, "Perturbation approach applied to modal diffraction methods," *J. Opt. Soc. Amer. A, Opt. Image Sci.*, vol. 28, no. 5, pp. 859–867, May 2011.

- [20] H. Wakabayashi, J. Yamakita, K. Matsumoto, and M. Asai, "Analysis of infinitely thin dielectric gratings with surface relief," *Electron. Commun. Jpn. Pt., Electron.*, vol. 82, no. 12, pp. 38–47, Dec. 1999.
- [21] P. Lalanne and D. Lemerrier-Lalanne, "Depth dependence of the effective properties of subwavelength gratings," *J. Opt. Soc. Amer. A, Opt. Image Sci.*, vol. 14, no. 2, pp. 450–458, 1997.



JIE LI was born in Hunan, China, in 1996. He received the B.S. degree in camouflage engineering from the Army Engineering University of PLA, Nanjing, China, in 2018, where he is currently pursuing the Ph.D. degree with the National Key Laboratory on Electromagnetic Environmental Effects and Electro-Optical Engineering. His current research interest includes computational electromagnetics.



JIAN-BAO WANG was born in Shandong, China, in 1983. He received the B.S. degree in mechanical engineering and automation and the Ph.D. degree in armament science and technology from the PLA University of Science and Technology, Nanjing, China, in 2005 and 2014, respectively.

He is currently an Associate Professor with the National Key Laboratory on Electromagnetic Environmental Effects and Electro-Optical Engineering, Army Engineering University of PLA, Nanjing, China. His research interest includes computational electromagnetics.



ZHENG SUN received the B.S. degree in automatic control from Southeast University, Nanjing, China, in 2009, and the Ph.D. degree in electrical engineering from the PLA University of Science and Technology, Jiangsu, China, in 2014.

He is currently working as a Lecturer with the National Key Laboratory on Electromagnetic Environmental Effects and Electro-Optical Engineering, Army Engineering University of PLA, Nanjing, China. His research interests include computing electromagnetics and lightning protections.



LI-HUA SHI (Member, IEEE) received the B.S.E.E. degree in electronics engineering from Xidian University, Xi'an, China, in 1990, the M.S. degree in electrical engineering from the Nanjing Engineering Institute, Nanjing, China, in 1993, and the Ph.D. degree in instrument science from the Nanjing University of Aeronautics and Astronautics, Nanjing, in 1996.

In 2001, he was a Visiting Scholar at Stanford University. He is currently a Professor with the National Key Laboratory on Electromagnetic Environmental Effects and Electro-Optical Engineering, Army Engineering University of PLA, Nanjing. His current research interest includes time-domain measurement technology.

Dr. Shi is a member of IEEE's Instrumentation and Measurement Society and Electromagnetic Compatibility Society. He was a recipient of three awards from the Ministry of Science and Technology of China.



YAO MA was born in Jiangsu, China, in 1984. She received the B.S. degree in electronics information engineering from Suzhou Science and Technology University, Suzhou, China, in 2006, and the M.S. degree in electromagnetic field and microwave technology from Southeast University, Nanjing, China, in 2009. She is currently pursuing the Ph.D. degree in armament science and technology with the Army Engineering University of PLA, Nanjing.

Her research interests include computational electromagnetics and metamaterials.



QI ZHANG was born in Shandong, China, in 1987. He received the M.S. and Ph.D. degrees from the PLA University of Science and Technology, Nanjing, China, in 2012 and 2015, respectively.

He is currently a Lecturer with the National Key Laboratory on Electromagnetic Environmental Effects and Electro-Optical Engineering, Army Engineering University of PLA, Nanjing. His research interests include lightning observation and computational electromagnetics.



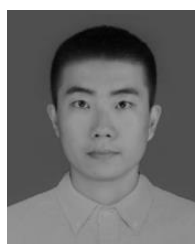
SHANG-CHEN FU received the B.E. degree in electrical engineering and automation from the PLA Aviation School, Beijing, China, in 2009, and the Ph.D. degree from the PLA University of Science and Technology, Nanjing, China, in 2015.

He is currently a Lecturer with the National Key Laboratory on Electromagnetic Environmental Effects and Electro-Optical Engineering, Army Engineering University of PLA, Nanjing, China. His research interests include structural health monitoring (SHM) and the lightning strike protection of composites.



YI-CHENG LIU was born in Yunnan, China, in 1995. He received the B.S. degree in electronics and information science and technology from Sichuan University, Chengdu, China, in 2017, and the M.S. degree in electronic science and technology from the Army Engineering University of PLA, Nanjing, China, in 2019.

His current research interest includes computational electromagnetics.



YU-ZHOU RAN was born in China, in 1994. He received the B.S. degree in electronic science and technology from Chongqing University, Chongqing, China, in 2016, and the M.S. degree in electromagnetic field and microwave technology from Air Force Engineering University, Xi'an, China, in 2018. He is currently pursuing the Ph.D. degree in armament science and technology with the Army Engineering University of PLA, Nanjing, China.

His current research interests include metamaterials, and metasurfaces and their applications to multifunctional devices.

...